DELAYED INCREASE IN CONE PENETRATION RESISTANCE OF SAND AFTER DYNAMIC COMPACTION

R.L. Michalowski
Department of Civil and Environmental Engineering, University of Michigan, Ann Arbor, USA

S.S. Nadukuru
Department of Civil and Environmental Engineering, University of Michigan, Ann Arbor, USA

ABSTRACT: *Among soil improvement techniques used to increase strength of loose and medium-dense sand deposits are the dynamic means, such as vibrocompaction and blasting. Sands often exhibit a drop in cone penetration resistance immediately after the disturbance, but a gradual increase in the resistance occurs in a matter of weeks and months. An explanation of the former is sought in the analysis of the stress state immediately after the dynamic disturbance, and a justification for the latter is found in the process of stress corrosion cracking (or static fatigue) of the micro-morphologic features at the contacts between sand grains. Some experimental evidence is demonstrated for fracturing of the microscopic features on the sand contact surfaces. Discrete element method calculations are carried out to strengthen the hypothesis, and the results of finite element analysis are demonstrated to provide quantitative estimates for the time-delayed increase in the sand penetration resistance.*

1 INTRODUCTION

Sand deposits subjected to densification through dynamic means (blasting, vibrocompaction) often exhibit a drop in cone penetration resistance immediately after compaction. However, the resistance to cone penetration increases over time, far beyond the time needed for the excess pore water pressure to dissipate. An early description of this peculiar behavior was given by Mitchell & Solymar (1984), confirmed by the data from a hydroelectric project in Nigeria. Blasting was found to reduce the penetration resistance immediately afterwards, even though the densification was evident by the surface subsidence. A considerable increase in penetration resistance, however, was found after 11 weeks. A similar effect was found after vibro-compacting sand on the same project. More examples of this phenomenon can be found in Baxter (1999). Mineral dissolution and cementation at interparticle contacts developed in time after dynamic compaction was cited first as a primary reason for the time-delayed increase in cone penetration resistance. More recently, this argument was dropped as the major cause of this peculiar effect, but the behavior is still referred to as a "continuing *Enigma*" (Mitchell, 2008).

A hypothesis is suggested, indicating that the cause of the time-delayed increase in penetration resistance of sand after dynamic compaction is the change in the stress state caused in the sand by the change of its stiffness (in particular, the change in elastic properties). An increase in elastic moduli at the macroscopic scale is caused by the process of micro-fracturing of the morphological features on the surfaces of grains at their contacts. This is a time-delayed process that can be accelerated by environmental factors (such as moisture), and often referred to as *stress corrosion cracking*. It will be argued that in confined sands this process brings the grains closer together (*grain convergence*), producing an increase in contact stiffness that manifests itself at the macro scale as an increase in elastic moduli. An evidence for delayed increase in elastic moduli of sand can be found in the results presented by Afifi & Woods (1971), who demonstrated that the velocity of the shear wave propagation increases in sands subjected to prolonged loading. As a consequence of the change in elastic moduli, the horizontal stress in a sand bed (under one-dimensional deformation conditions) will increase, leading to an increase in the cone penetration resistance. Changing stress state was mentioned earlier in the literature as a direct cause of this increase (Schmertmann, 1987); here, we suggest a hypothesis why the change in the stress state occurs.

Particle "rearrangement" and "structuration" are often cited as sources of changes in granular assemblies leading to variation in properties (Mesri et al., 1990; Bowman and Soga, 2003), and they have been used to explain the puzzling effect of delayed increase in cone penetration resistance in dynamically compacted sands. Rearrangement of particles and restructuring, however, are the results of an underlying process, and cannot be considered as causes of this mystifying behavior. A hypothesis presented in this paper places emphasis on the time-delayed micro-fracturing of the morphological features at grain surfaces. The evidence available in the literature to support this hypothesis is discussed and numerical simulations are used to complement this evidence.

2 STATIC FATIGUE AT GRAIN CONTACTS

The micro-morphology of grain surfaces is illustrated in Fig. 1. When two particles with a rich surface morphology come into contact, it is the asperities and the small crystalline fragments that are first loaded to a considerable degree as the areas of the surfaces in contact are relatively small (*microstress*).

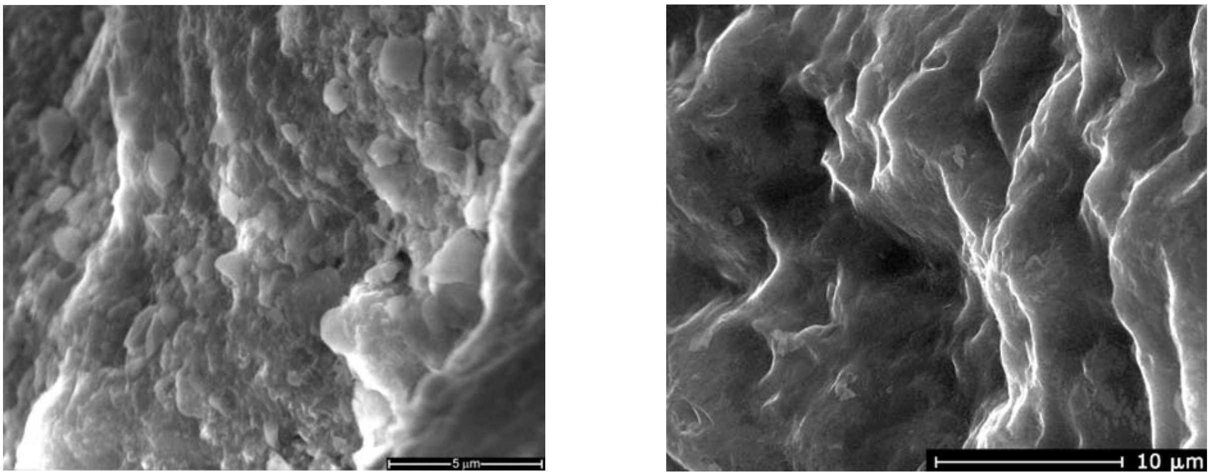

(a) (b)

Fig. 1. Micro-morphology of sand grain surfaces: (a) Michigan Lake dune sand, and (b) Ottawa 20-30 sand

Consequently, the microscopic features on the contacts are prone to develop cracks in time, the process called *stress corrosion cracking*. Because this process is time-delayed, it is often termed *static fatigue*. Micro-fracturing does not occur simultaneously at all contacts, and presumably, takes place with different intensity at different contacts, depending on the current distribution of the force chains. This hypothesis was suggested recently by Michalowski & Nadukuru (2010, 2011a, 2011b).

In an effort to gain evidence for this time-delayed fracturing, an experiment was performed where three grains placed in a triangular pattern were loaded with a total load of about 2.1 N. The load was transmitted to the grains through a glass plate. Surface morphology of the grains was inspected using scanning electron microscopy before the start of the test, 15 minutes after the load was applied, and after one week. Scanning electron imaging was used to identify regions of fracturing. A set of pictures for one grain is shown in Fig. 2.

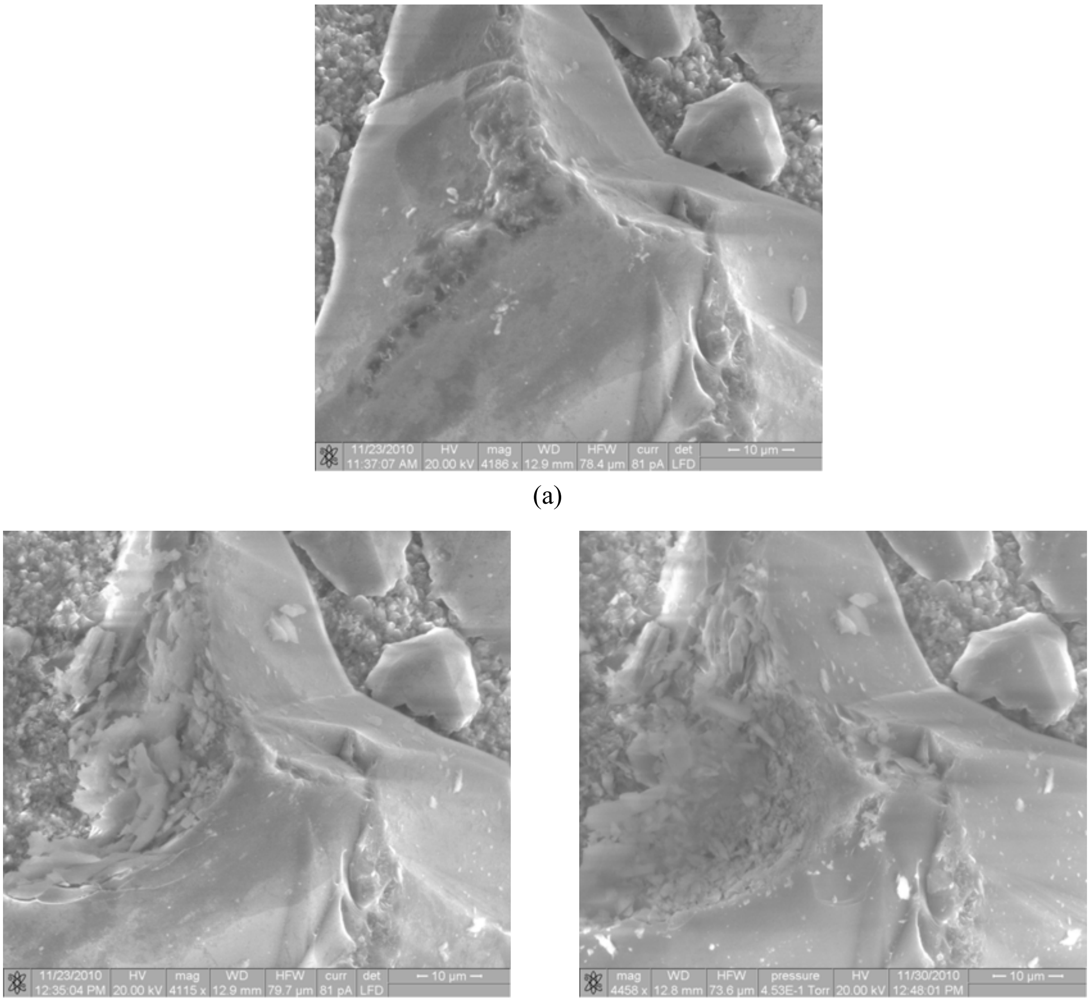

(a)

(b) (c)

Fig. 2. Fracturing of quartz asperity: (a) before loading, (b) after 15 min. of loading, and (c) after one week

A microscopic view of a quartz asperity on the grain surface prior to testing is shown in Fig. 2(a); the width of the picture is about 70 μm. Fractured (crushed) asperity, after 15 min of loading, is shown in Fig. 2(b), with the debris deposited on the fracture surface. It is not clear whether all this fracturing occurred immediately after application of the load or was distributed in the 15-min period. The fractured zone expanded during the following week is illustrated in Fig. 2(c). Continuing fracturing is quite noticeable (the load was kept constant and equal to that in the first 15 minutes of the test).

Static fatigue is not a new concept, but only recently was it used to explain mechanical behavior of sand by Lade & Karimpour (2010a, 2010b), who considered static fatigue of grains (delayed grain fracturing). Static fatigue has been considered in material science for decades (Charles, 1958) as a time-dependent fracturing process in brittle materials. Scholz

(1968, 1972) reviewed experimental work on creep of rocks, and concluded that, at low temperatures and pressure, the primary mechanism of creep of brittle rocks is delayed micro-fracturing.

3 STRESS CHANGE IN SOIL BED AFTER DYNAMIC COMPACTION

First, the development of the stress state in freshly compacted sand is discussed, followed by discrete element simulations and energy considerations.

3.1 Dynamic disturbance and post-liquefaction stress state

Compaction of sand requires a change in its packing, so that the volume of pores can be reduced. When saturated sands are dynamically compacted, the contact forces between grains are lost (liquefaction) and reconfigured, so that a tighter packing can be achieved. The effective stresses are reduced to zero during liquefaction, but the stress state is rebuilt upon dissipation of the excess pore water pressure. The vertical macroscopic stress is governed by gravity. When the effective vertical macroscopic stress increases from zero during liquefaction to a value that balances the buoyant weight of the soil at any depth, the horizontal stress will trail with its value such, so that the stress state is just below the yield condition of the newly compacted sand. This horizontal stress is then likely to be significantly lower than the stress in the pre-liquefaction sand bed that was subjected to long-term gravity loads. To demonstrate that this conjecture is reasonable, we perform discrete element simulations.

3.2 DEM calculations

To illustrate the process of liquefaction and subsequent re-building of the stress state, discrete element simulation is carried out. An assembly of over 11 thousand grains was generated using the *PFC*^{3D} (2008) computer code, Fig. 3. These grains were predominantly spherical with radii between 2.3 and 3.7 cm. 25% of the grains were in the form of “clumps” (particles with a shape of two overlapping spheres with the centers offset by one radius, *i.e.*, peanut-shape particles, shown darker in Fig. 3).

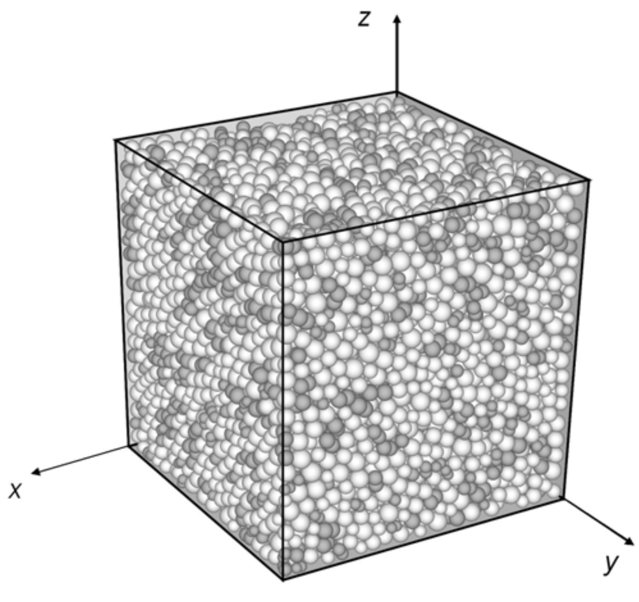

Fig. 3. An assembly of particles used in DEM simulations

The assembly was formed in a cube of 1.2 m in size, with initial porosity of 0.35. The contact normal and tangential stiffness was set to $K_n = 4.0$ and $K_t = 1.6$ MN/m, respectively, and the coefficient of grain interface friction μ = 0.65 was used, or contact friction angle of 33° (mass density of the grains was 2,650 kg/m^3 and gravity acceleration was taken as 9.81 m/s^2). The ratio of horizontal-to-vertical macroscopic stress in the prepared specimen was $k = 0.473$. A numerical triaxial compression test of the specimen was then simulated with a confining pressure of 50 kPa. Interpreting the strength of the granular assembly as frictional with a linear envelope, the peak internal friction angle was found to be 33.5°.

Liquefaction simulations using DEM with two-phase medium are rarely attempted, but the phenomenon resembling liquefaction can be simulated using a granular assembly without modeling the pore fluid. The central phenomenon to liquefaction is loss of inter-granular contacts; this loss of contacts was simulated by reducing the grains' diameter by fraction 0.001. This change had no significant effect on the porosity. An alternative one-phase method of inducing liquefaction is through a constant-volume cyclic strain process of the granular assembly (Ng & Dobry, 1994). The latter was not used, because it requires zero gravity condition, whereas gravity is crucial to the simulation of stress state formation after liquefaction.

Once new contacts were formed after simulated liquefaction, the effective stress state in the granular assembly was regained. Stiffness of newly-formed contacts was taken at half of the originally used value, to reproduce the low stiffness of contacts that have not yet been subjected to *stress corrosion cracking*. The (effective) macroscopic stress state was regained with the vertical stresses governed by gravity, with the horizontal stress significantly lower than the pre-liquefaction value, leading to the horizontal-to-vertical stress ratio of $k = 0.339$ ($k = 0.473$ prior to liquefaction). This process occurred without a change in porosity, and the numerically tested internal friction angle was practically unchanged (33.6°).

Table 1. Increase in stress ratio k (1-D strain) as function of an increase in inter-granular elastic stiffness (DEM simulation)

K_n (MN/m)	K_s (MN/m)	k
2.0	0.8	0.339
2.2	0.88	0.365
2.4	0.96	0.378
2.6	1.04	0.391
2.8	1.12	0.399
3.0	1.2	0.413
3.2	1.28	0.424
3.4	1.36	0.433
3.6	1.44	0.442
3.8	1.52	0.451
4.0	1.6	0.459

In time, under one-dimensional strain conditions, static fatigue at inter-granular contacts will lead to *grain convergence* and an increase in contact stiffness. This increase was simulated in ten equal steps. The stress ratio increased gradually, up to the value of $k = 0.459$ (Table 1), which is close to the pre-liquefaction ratio of 0.473. At this time no experimental data exists to assess the rate at which the contact stiffness increases; observations indicate that it might be the order of months (dependent on the level of loading).

3.3 Anisotropy of elastic properties and energy argument

Preliminary numerical testing using DEM indicates that the averaged elastic properties of a granular assembly consolidated under gravity conditions are cross-anisotropic. Elastic macroscopic properties are then described with five material constants: two Young's moduli and three Poisson's ratios.

A macroscopic analysis was attempted for predicting the change in the stress ratio (under one-dimensional strain conditions) with the change in the elastic stiffness caused by static fatigue. This was done using the energy balance equation applied to a soil column. Denoting the initial stress ratio by k_1, the stress ratio after the stiffness increase is described as k_2 in the following equation

$$k_2 = \sqrt{\frac{\frac{E_h'}{E_h}(1-\nu_{hh})\,k_1^2 - \frac{1}{2}\left(\frac{E_h'}{E_v} - \frac{E_h'}{E_v'}\right) + \xi(1-\chi)E_h'}{1-\nu_{hh}'}} \tag{1}$$

where E and ν are the Young moduli and Poisson's ratios, and subscripts v and h pertain to vertical and horizontal directions, respectively. The *primed* values of the elastic parameters are the altered ones by the process of static fatigue. The details of this analysis will be presented elsewhere (Michalowski & Nadukuru, 2011a).

When energy balance is used, one needs to estimate the macro-strain due to grain convergence, and the amount of energy dissipated ("used") in the process of stiffness increase. The strain due to grain convergence was assumed proportional to the depth (*i.e.*, proportional to the stress caused by gravity); this is embedded in coefficient ξ, with its value estimated at 10^{-6} - 10^{-5} (kPa^{-1}). Recent microscopic studies indicate that this value may be higher. Information about the amount of energy needed for the process of stiffness increase is contained in coefficient χ. This coefficient determines the dissipated energy as a portion of the gravity work done on grain convergence.

Calculations with eq. (1) were carried out for a sand bed with anisotropic macroscopic elastic properties obtained from numerical simulations on a grain assembly in Fig. 3. Coefficients ξ and χ were assumed to be $1.25 \cdot 10^{-5}$ and 0.2 (or 20%), respectively. Starting from the initial stress ratio of $k_1 = 0.339$, the value of 0.462 was obtained for k_2 from eq. (1), quite close to the DEM-simulated value of 0.459 (Table 1). While the energy approach contains two well-defined, but only approximately estimated parameters (ξ and χ), the preliminary result indicates that it may be a reasonable method of analysis.

4 SIMULATION OF CONE PENETRATION RESISTANCE

The hypothesis suggested here is that the initial drop in the cone penetration resistance after dynamic compaction is due to the change of the stress state caused by liquefaction. The post-liquefaction stress state is characterized by the horizontal stress lower than that in pre-liquefaction sand bed. This causes the deviatoric stress to increase, producing the stress state that is closer to the yield condition than the pre-liquefaction stress state. Subsequently, increase in the horizontal stress caused gradually by the process of stiffness increase, contributes to the time-delayed increase in the cone penetration resistance.

Finite element simulations of this process were attempted. Rather than simulating a continuous process of cone penetration, an analysis was carried out of on a block shown schematically in Fig. 4. The depth was simulated by the effective stress condition (σ_v) at the top boundary, but the soil in the block was considered weightless.

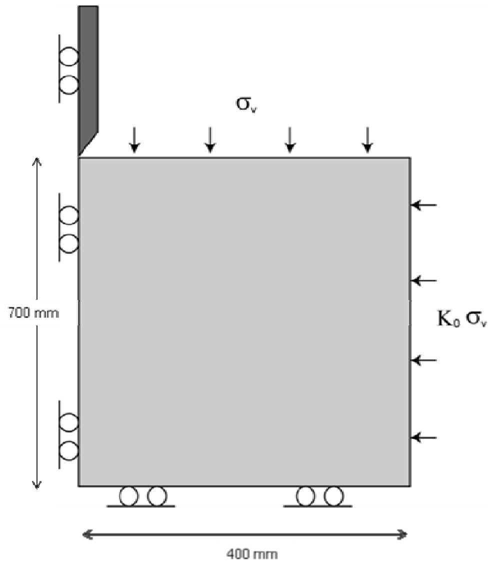

Fig. 4. Boundary conditions for FEM simulations of the cone penetration process, with depth adjusted by the stress condition on the top boundary

The analysis was carried out using Abaqus/CAE ver 6.10. The soil and cone were modeled with axisymmetric four-node elements, and the explicit solution scheme was used.

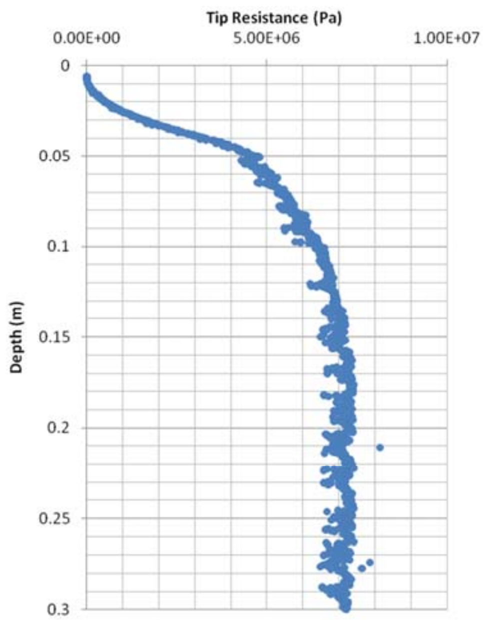

Fig. 5. Increase in cone penetration resistance with depth; steady-state resistance was taken as the value at the depth related to the stress condition at the top boundary of the simulation block

Adaptive meshing technique was utilized. The coefficient of friction between the cone and soil was assumed to be 0.3. The yielding of the soil was modeled with the Drucker-Prager criterion and the deformation was governed by the non-associative flow rule (nearly incompressible). The details of the analysis will be presented elsewhere; here, we only use the results of the analysis as an argument for the hypothesis of variation of the stress being the primary cause of the drop and then increase in the cone penetration resistance after dynamic compaction of sands.

A typical graph of the cone resistance vs. penetration depth is illustrated in Fig. 5. The soil is characterized here by the friction angle of ϕ = 37° and the effective vertical stress at the top boundary is taken as σ_v' = 0.25 MPa (and k_1 = 0.39), which represents the stress at the depth of about 15 m. The soil in the model in Fig. 4 is weightless, and the steady-state value in Fig. 5 is taken as the cone penetration resistance at the depth set by the stress boundary condition. An example of the vertical and horizontal stress distribution in the neighborhood of the cone tip is presented in Fig 6.

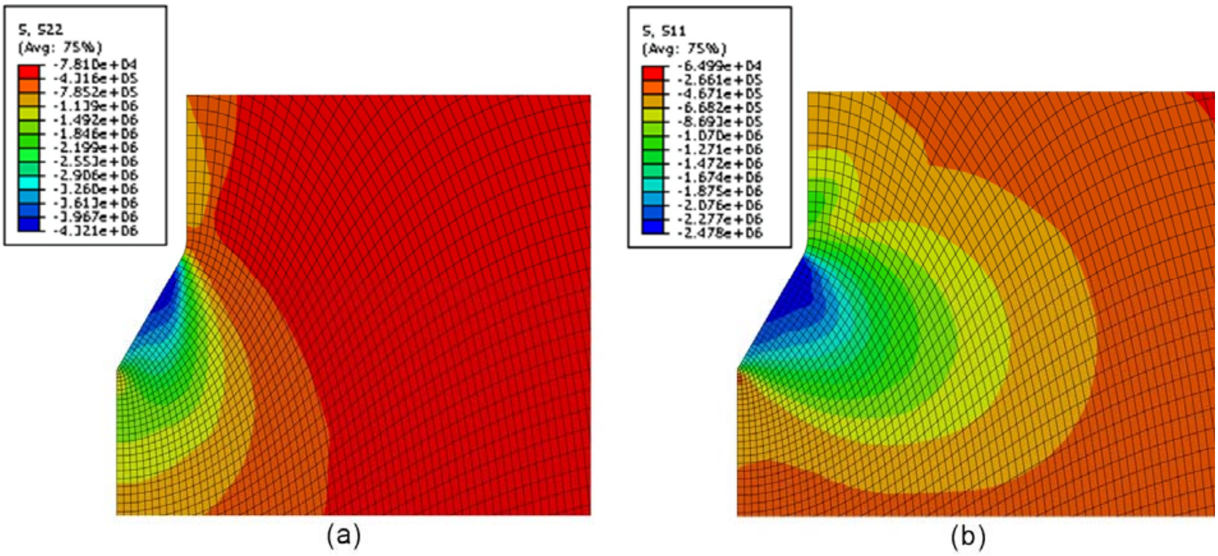

Fig. 6. Stress distribution in proximity of the cone tip: (a) vertical stress, and (b) horizontal stress

The initial horizontal-to-vertical stress ratio was taken as k_1 = 0.33. The consequence of an increase in soil stiffness (caused by grain convergence) is an increase in coefficient of earth pressure k. However, the relationship of the soil stiffness and k is not a material relationship; rather, it is the result of the loading history and the process of static fatigue. Triaxial tests were simulated numerically using PFC^{3D} (Fig. 3) to indicate how the stress ratio k changes with an increase in the inter-granular stiffness. These results were shown in Table 1, and the penetration resistance is simulated here for the stress ratio changing from 0.33 to 0.45.

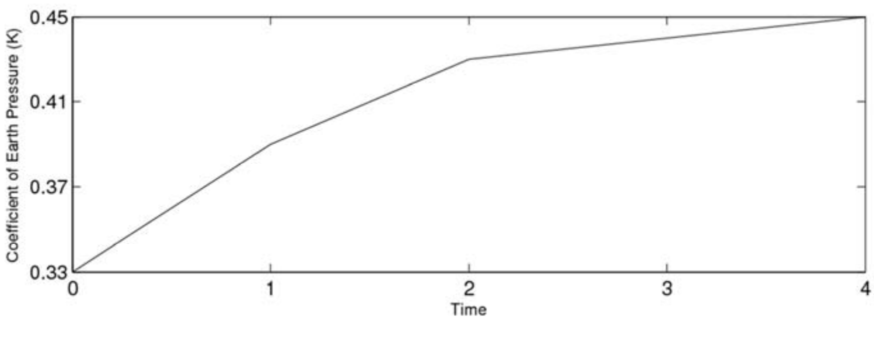

Fig. 7. Assumed increase in stress ratio k as function of time

Because the time-dependent increase in the soil stiffness (and, consequently, increase in ratio k) is still a subject of investigation, we assume the the change in k as in Fig. 7, with intervals 1 through 4 representing time. The blue line (without number designation) in Fig. 8 shows the cone penetration resistance calculated for a soil bed with internal friction angle of $\phi = 32°$ and $k = 0.45$ (the state prior to compaction).

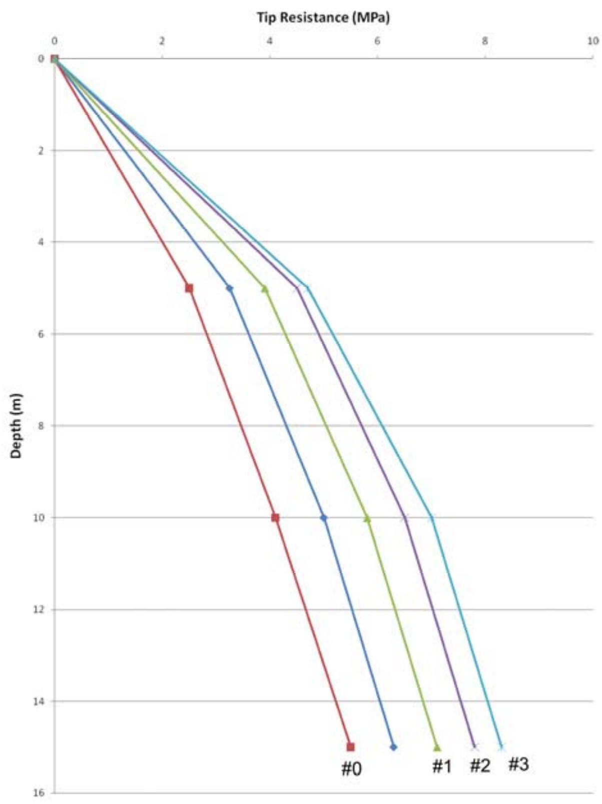

Fig. 8. FEM simulation results of cone penetration resistance

At the time of dynamic compaction the soil bed is liquefied, and the re-gained effective stress state is characterized with a low k of 0.33. Although the sand was assumed to be compacted with the internal friction angle increasing from 32° to 37°, the penetration resistance decreased (red line, #0); such is the impact of the drop in the horizontal stress. The decrease in the horizontal stress caused an increase in the deviatoric stress, moving the stress (in the stress space) closer to the failure surface. After the first time interval (0 to 1 in Fig. 7), the penetration resistance increased to reach the line marked as #1 in Fig. 8, and in the two subsequent intervals the resistance increased as indicated by lines #2 and #3. It is evident that the delayed increase in the cone penetration resistance can be caused by a gradual change in the stress state in the compacted soil and not by an increase in the soil strength. In pressure-dependent soils, of course, the shear strength is dependent on the first invariant of the stress state.

Changes in the stress state in the soil bed after dynamic compaction were considered earlier by Schmertmann (1987, 1991) as a possible cause of the delayed increase in soil penetration resistance. This cause was also alluded to by Mesri et al. (1990). The process of *static fatigue* and *grain convergence* described in this paper explains the mechanism of the delayed response of the sand bed after dynamic compaction.

5 CONCLUSIONS

While much research has been published regarding the peculiar behavior of sand deposits after dynamic compaction, no convincing explanation for the delayed increase in cone penetration resistance was presented. This paper indicates the hypothesis of *static fatigue* as the cause of that behavior. Numerical simulations seem to support this hypothesis. To gain information on the time scale of the process, further experimental research is needed, with the focus on the rate of static fatigue as a function of the stress state and environmental factors (moisture).

ACKNOWLEDGEMENT

The work presented in this paper was supported by the National Science Foundation through grant CMMI-0724022, and by the Army Research Office, grant No. W911NF-08-1-0376. This support is greatly appreciated. The authors also would like to thank Itasca Consulting Group for academic license of their PFC^{3D} code, and The University of Michigan Electron Microbeam Analysis Laboratory for the use of their Quanta 3D Scanning Electron Microscope supported by the National Science Foundation, grant No. DMR-0320740.

REFERENCES

Afifi, S.S. & Woods, R.D. (1971). "Long-term pressure effects on shear modulus of soils." ASCE J. Soil Mech. Found. Div., Vol. 97(10), 1445-1460.

Baxter, C.D.P. (1999). An Experimental Study on the Aging of Sands. Ph.D. Dissertation, Virginia Tech (Virginia Polytechnic Institute and State University), Blacksburg, VA.

Bowman, E.T. & Soga, K. (2003). "Creep, ageing and microstructural change in dense granular materials." Soils and Foundations, Vol. 43(4), 107-117.

Charles, S.J. (1958). "Static fatigue of glass. I." Journal of Applied Physics, Vol. 29(11), 1549-1553.

Lade, P.V. & Karimpour, H. (2010a). "Static Fatigue Controls Particle Crushing and Time Effects in Granular Materials." Soils and Foundations, Vol. 50(5), 573-583.

Lade, P.V. & Karimpour, H. (2010). "Static fatigue produces time effects in granular materials." ASCE Proc.: Advances in Analysis, Modeling and Design, GeoFlorida, Feb. 20-24, 2010.

Mesri, G., Feng, T.W. & Benak, J.M. (1990). "Postdensification penetration resistance of clean sand." J. Geotech. Eng., Vol. 116(7), 1095-1115.

Michalowski, R.L. & Nadukuru, S.S. (2010). "Stress corrosion cracking and relaxation of deviatoric stress after dynamic compaction of sand." 37th Solid Mechanics Conference, (SolMech 37), Keynote, Sept. 6-10, 2010, Warsaw, Poland (extended abstract).

Michalowski, R.L. & Nadukuru, S.S. (2011a). "Static fatigue and relaxation of deviatoric stress after dynamic compaction of sands." J. Geotech.Geoenv. Eng., in review.

Michalowski, R.L. & Nadukuru, S.S. (2011b). "Stress corrosion cracking and multi-scale process of delayed increase in penetration resistance after dynamic compaction of sand." Geo-Frontiers 2011, March 13-16, 2011, Dallas, TX.

Mitchell, J.K. & Solymar, Z.V. (1984). "Time-dependent strength gain in freshly deposited or densified sand." J. Geotech. Eng., Vol. 110(11), 1559-1576.

Mitchell, J.K. (2008). "Aging of sand – a continuing enigma?" Proceedings of the 6th Int. Conf. on Case Histories in Geotechnical Engineering. Arlington, VA, Aug. 11-16, 2008, 1-21.

Ng, T.T. & Dobry, R. (1994). "Numerical simulations of monotonic and cyclic loading of granular soil." Journal of Geotechnical Engineering, Vol. 120(2), 388-403.

PFC3D. (2008). *Particle Flow Code in 3 Dimensions*. Itasca Consulting Group, Inc. Minnepolis, MN.

Schmertmann, J.H. (1987). "Time-dependent strength gain in freshly deposited or densified sand." Discussion, J. Geotech. Eng. Vol. 113(2), 173-175.

Schmertmann, J.H. (1991). "The mechanical aging of soils." J. Geoecht. Eng., Vol. 117(9), 1288-1330.

Scholz, C.H. (1968). "Mechanism of creep in brittle rock." J. Geophys. Res., Vol. 73(10), 3295-3302.

Scholz, C.H. (1972). "Static fatigue of quartz." J. Geophys. Res., Vol. 77(11), 2104-2114.